Equilibrium Folding Studies of Tetrameric R67 Dihydrofolate Reductase†

Ping Zhuang,‡ Edward Eisenstein,§ and Elizabeth E. Howell*,‡

Biochemistry Department, University of Tennessee, Knoxville, Tennessee 37996-0840, and Center for Advanced Research in Biotechnology, Rockville, Maryland, and Department of Chemistry and Biochemistry, University of Maryland Baltimore County, Baltimore, Maryland 21229

Received October 11, 1993; Revised Manuscript Received February 9, 1994®

ABSTRACT: R67 dihydrofolate reductase (DHFR) is an R-plasmid encoded enzyme that confers resistance to the antibacterial drug trimethoprim. This enzyme is not homologous in sequence or structure to chromosomal DHFRs. Equilibrium folding of tetrameric R67 DHFR was studied and found to be fully reversible. Formation of an inactive intermediate was assayed by loss of enzyme activity. Denaturation of the intermediate was monitored by concurrent changes in fluorescence and circular dichroism signals. Both transitions are protein concentration dependent. A simple model fitting these data is tetramer $\rightleftarrows$ 2 dimers $\rightleftarrows$ 4 unfolded monomers. No evidence for folded monomer was found. Global fitting of all the folding data yielded a ΔG_{H_2O} of −9.63 kcal/mol for the initial transition and a ΔG_{H_2O} of −12.35 kcal/mol for the second transition. In addition, thermal unfolding of tetrameric R67 DHFR was found to be reversible. A folding intermediate also occurred during thermal unfolding as evidenced by the asymmetric endotherms and a $\Delta H_{calorimetric}/\Delta H_{van't\ Hoff}$ ratio of 2.1.

A fundamental question in biochemistry is how the primary sequence of a protein is transduced into a tertiary or quaternary structure. In other words, how do proteins fold? While substantial progress has been made in addressing this problem, a set of rules delineating a protein folding code has not yet been determined. Current studies indicate that refolding is a sequential, cooperative process, with a "random coil" structure initially folding to a "molten globule" state possessing a high degree of structure but substantial mobility (Kuwajima, 1989). Molten globule formation is facilitated by either hydrophobic interactions and/or secondary structure formation. Other intermediates may occur prior to formation of the native structure, for example, forms which contain cis isomers of X–proline peptide bonds (Schmid, 1992). Detailed descriptions of folding intermediates are, in general, lacking.

Other deficiencies in our understanding of protein folding stem from the relatively few detailed investigations of predominately β-sheet proteins and oligomeric proteins. The latter couples the inherent complexity of protein folding with subunit association (Jaenicke, 1991; Janin, 1991). To provide a model system for folding studies in a tetrameric, β-sheet enzyme, we have initiated folding studies in R67 dihydrofolate reductase (DHFR),[1] an R-plasmid encoded enzyme that is not homologous to chromosomal DHFRs either in sequence or structure. Of especial interest, each monomer in R67 DHFR is only 78 amino acids long, making this one of the smallest enzymes known to assemble into an active quaternary structure.

Each monomer in R67 DHFR is a β-barrel with the fifth strand missing (Matthews et al., 1986). Two monomers in R67 DHFR associate to form a dimer, with three strands from each monomer meshing to form a six-stranded β-barrel at the subunit interface. Two dimers associate to form the catalytically active tetramer. Each monomer in the X-ray structure of tetrameric R67 DHFR has electron density for residues 17–78[2] (Narayana, Xuong, and Matthews, personal communication).

Two tryptophans occur per monomer in R67 DHFR; their positions in dimeric R67 DHFR are shown in Figure 1. W45 and W145, as well as the symmetry related residues W245 and W345, occur at the monomer–monomer interfaces. W38 and W338 (and W138 and W238) occur at the dimer–dimer interfaces. Use of the crystallographic 222 symmetry operator (star in Figure 1; Matthews, Xuong, and Narayana, personal communication) on monomeric R67 DHFR generates tetrameric R67 DHFR.

In R67 DHFR, we have the advantage of altering folding and association complexity as a function of pH. At pH 5.0, R67 DHFR is dimeric and equilibrium folding has been found to be a two-state process (Reece et al., 1991). However, with increasing pH, dimeric R67 DHFR undergoes a pH-dependent association to form tetramer (Nichols et al., 1993). Our equilibrium folding studies on tetrameric R67 DHFR at pH 8.0 are described below. Initial studies indicate that R67 DHFR undergoes reversible thermal and chemical denaturation at pH 8; however, folding is no longer a two-state process as an intermediate occurs.

MATERIALS AND METHODS

Equilibrium Folding Studies of Tetrameric R67 DHFR at pH 8.0. Unfolding of tetrameric R67 DHFR[3] using the chemical denaturant guanidine hydrochloride (GdnHCl) was monitored using fluorescence and circular dichroism techniques as previously described (Reece et al., 1991; Zhuang et

† This research was supported in part by NIH Grant GM35308 (to E.E.H.) and NSF Grant DMB90-02177 (to E.E.).

‡ University of Tennessee.

§ Center for Advanced Research in Biotechnology and University of Maryland Baltimore County.

® Abstract published in *Advance ACS Abstracts,* April 1, 1994.

[1] Abbreviations: R67 DHFR, R67 dihydrofolate reductase; T, tetramer; D, dimer; M, folded monomer; U, unfolded monomer; GdnHCl, guanidine HCl; CD, circular dichroism; bis-ANS, 1,1′-bis(4-anilino-5-naphthalenesulfonic acid); MTH buffer, 100 mM Tris + 50 mM MES + 50 mM acetic acid polybuffer.

[2] The amino acids in the first monomer are labeled 17–78; those in the second monomer, 117–178; the third monomer, 217–278; and the fourth monomer, 317–378. For brevity, when a single residue is mentioned in the text, all four residues are implied.

[3] Protein concentrations are expressed as tetramer unless specified otherwise.

0006-2960/94/0433-4237$04.50/0

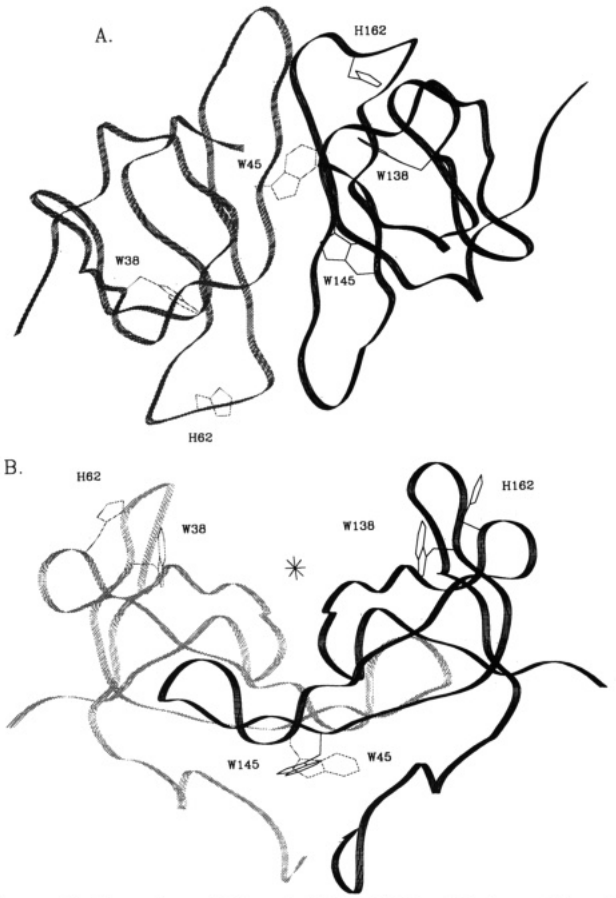

FIGURE 1: Two views of dimeric R67 DHFR with the position of histidine and tryptophan residues indicated (Matthews et al., 1986). Monomer 1 is light gray and monomer 2 is black. An approximately 90° rotation along the x axis generates panel A from panel B. W45 and W145 occur at the monomer–monomer interfaces. In panel B, a 222 symmetry element (star) relates the monomer of R67 DHFR to tetrameric R67 DHFR (Matthews, Xuong, and Narayana, personal communication). The environment of W38, W138 as well as H62, H162 can be envisioned to become buried in tetrameric R67 DHFR by a 180° rotation along the z axis using the symmetry element (star). The star is positioned at the center of the active site pore.

al., 1993). In brief, a Perkin-Elmer LS-5B was employed for fluorescence studies; tryptophans were excited at 290 nm and emission monitored at 340 nm using a cell path length of 1 cm. For circular dichroism studies, spectra at room temperature were obtained using either a Jasco 40A or a Jasco J720 spectropolarimeter. The cell path length was 2 mm. Ten spectra were acquired per sample using 1-nm steps and 2-s integrations and an averaged spectrum calculated for the Jasco J720 data. Only two scans were acquired for the Jasco 40A (6-s integrations), and averaged values were used. An essentially flat buffer baseline scan was then subtracted from the average protein scan to obtain the data presented below. GdnHCl concentrations were calculated using an equation relating refractive index to concentration (Pace et al., 1990) and refractive indexes were measured using a Zeiss refractometer.

Enzyme activity was monitored at 30 °C and initial rates of either a 1/63 or a 1/13.4 dilution from the GdnHCl solution were monitored. Enzyme-catalyzed rates for the first minute were linear, indicating that the presence of substrate and cofactor in the assay solution did not perturb the folding equilibria. Low concentrations of GdnHCl were added to control enzyme assays to test whether the presence of GdnHCl due to dilution from the unfolded enzyme stock could perturb the enzyme activity measurements. At the levels employed in our assays (≤0.3 M), GdnHCl did not affect activity measurements.

Sedimentation equilibrium studies using 5 μM protein were performed at ~20 °C with a Beckman-Spinco Model E ultracentrifuge as previously described (Nichols et al., 1993). Data were initially analyzed in terms of a single homogeneous species to obtain weight average molecular weights in the presence of increasing GdnHCl concentrations. In addition, data in the form of absorbance versus radius were further analyzed to obtain, where relevant, equilibrium constants relating the concentrations of monomer, dimer, and tetramer under a given set of experimental conditions, essentially as described by Nichols et al. (1993). Because of the high degree of correlation between the errors associated with the monomer–dimer and dimer–tetramer dissociation constants, however, an alternative method was used to assess the molecular species present in a particular experiment. In these cases, data were analyzed using an extension of the basic equation describing sedimentation equilibrium that includes additional terms for each potential species present. This equation is

$$A_{\text{total}} = B + \sum A_{\text{o,i}} \exp[iM_1(1 - \nu\rho)\omega^2(r^2 - r_{\text{o}}^2)/2RT] \quad (1)$$

where $A_{\text{o,i}}$ is the absorbance of the particular species (tetramer, dimers or monomer) at a reference position, r_{o} (e.g., for example, the meniscus), M_1 is the molecular weight of monomeric R67 DHFR (8430), ρ is the solvent density which was determined pychnometrically, ω is the angular velocity, r is the radial distance in centimeters from the center of rotation, R is the gas constant, T is the absolute (Kelvin) temperature, and B is a correction term for a nonzero baseline. A partial specific volume, υ, of 0.7159 mL/g was used for tetramer, dimer, and monomer, and it was assumed to be independent of denaturant concentration.

The number of species present under a given denaturant concentration was determined in this analysis by looking for a minimum in χ^2 for different models that included terms for additional components (i = 1, 2, or 4) in eq 1, corresponding to monomeric, dimeric, and tetrameric R67 DHFR species. For sedimentation equilibrium data in the presence of 2 M GdnHCl, it was surprising that a three species model, which gave the lowest χ^2 values and yielded excellent confidence intervals associated with the adjustable terms for the reference concentration of the particular protein species, yielded poor confidence intervals when the adjustable parameters were recast as equilibrium constants. Presumably this was due to the high correlation of error between monomer–dimer and dimer–tetramer dissociation constants. In spite of the large errors associated for the equilibrium constants, however, the two fits (e.g., for species or equilibrium constants) yielded identical χ^2 values.

For all studies at pH 8.0, overnight incubations of the protein in GdnHCl at room temperature were necessary to reach equilibrium. Folding was fully reversible as monitored by recovery of enzyme activity as well as fluorescence. Folding was not hysteretic as dilution of R67 DHFR from 6 M GdnHCl to an intermediate GdnHCl concentration resulted in equivalent fluorescence readings as unfolding dilutions.

Model Fitting. Folding in dimeric, reduced H62C R67 DHFR can be described by the two state process

$$\text{D} \overset{K}{\rightleftarrows} 2\text{U}$$

where D is dimer, U is unfolded monomer, and $K = [\text{U}^2]/[\text{D}]$. Denaturation data for this mutant R67 DHFR were fit to eq 4 in Reece et al. (1991) using a nonlinear least-squares fitting

program (NLIN) in the Statistical Analysis Systems program package (Sas Institute, Inc., Cary, NC).

Denaturation data for native, tetrameric R67 DHFR were fit to the three state model

$$T \overset{K_T}{\rightleftarrows} 2D \overset{K_D}{\rightleftarrows} 4U$$

where T is tetramer and $K_T = [D]^2/[T]$ and $K_D = [U]^2/[D]$. All enzyme activity, fluorescence, and CD unfolding data were fit globally using the computer program BIOEQS (Royer, 1993; Royer & Beechem, 1992). This program uses a numerical algorithm to solve simultaneous free energy equations and was generously made available by Dr. Royer. Confidence intervals are correlated with other parameters and are asymmetric. The ΔG_{H_2O} values and slopes were linked between the eight data sets. All values were allowed to vary initially. From an initial fit using 0.1 kcal/mol steps, a slope for the overall transition ($T \rightleftarrows 4U$) of 6.54 kcal mol^{-1} M^{-1} (4.78–6.82 kcal mol^{-1} M^{-1}, 67% confidence interval) was obtained. This slope was then fixed in subsequent fits with smaller steps to keep the free energy for the overall reaction sufficiently high so that minimal dimer would be predicted to be present in 0 M GdnHCl. This was done as previous studies indicated that substantial dimer does not occur at pH 8 using either sedimentation equilibrium or molecular sieving techniques (Nichols et al., 1993). The same approach was used to evaluate the data containing 60 μM NADPH. An initial fit using 0.1 kcal/mol steps yielded an overall slope of 7.46 kcal mol^{-1} M^{-1} (5.08–8.05 kcal mol^{-1} M^{-1}, 67% confidence interval). This overall slope was then fixed and smaller steps used in subsequent fits.

Differential Scanning Microcalorimetry. Thermal unfolding of native R67 DHFR was also studied using a Microcal MC-2D differential scanning microcalorimeter (DSC) between 20 and 95 °C. The instrument was operated using data acquisition and analysis programs (DA-2) supplied by the manufacturer. Samples were dialyzed extensively against 100 mM Tris + 50 mM MES + 50 mM acetic acid polybuffer (MTH, at pH 8.0) plus 5 mM dithiothreitol at 4 °C, and degassed for 10 min before use. The protein concentration was 148 μM tetramer. Scan rates were 1 °C per minute (up) and 0.5 °C per minute (down). Scans were repeated two times.

RESULTS

A Folding Transition Monitored by Enzyme Activity. Equilibrium folding of tetrameric R67 DHFR at pH 8.0 was monitored by enzyme activity measurements (Figure 2). The transition zone for unfolding/refolding is protein concentration dependent, indicating a bimolecular reaction is being monitored. Tetrameric R67 DHFR is the active catalytic species as our recent studies show dimer is only partially active due to loss of the active site pore (Nichols et al., 1993; Howell et al., in preparation). The folding curves in Figure 2 could describe an equilibrium between active tetramer and either dimers or folded monomers (i.e., $T \rightleftarrows 2D$ or $T \rightleftarrows 4M$). However the latter appears unlikely as fluorescence and CD techniques (below) monitor a second noncoincident transition that is protein concentration dependent. The CD/fluorescence data likely measure an equilibrium between dimers and unfolded monomers (see below).

Folding Transitions Monitored by Circular Dichroism and Fluorescence. Equilibrium folding curves monitored by CD are shown in Figure 3. These curves are also protein concentration dependent; however, the midpoints for the unfolding/refolding transitions occur at slightly higher GdnHCl concentrations than observed for the enzyme activity profiles. Observation of a different midpoint when the activity and CD data at a single protein concentration are compared indicates a folding intermediate is being monitored by CD. Since the change in θ at 217 nm is minimal when CD spectra for dimer (pH 5.0) and tetramer (pH 7.0) are compared (1.19 fold, dimer value ÷ tetramer value; Zhuang et al., 1993), we would not anticipate a biphasic folding curve. Thus the CD data appear transparent to the equilibrium between tetramer and two dimers and likely monitor the equilibrium between two folded dimers and four unfolded monomers. While the CD plots could contain some additional information about the tetramer $\rightleftarrows$ 2 dimers equilibrium, we believe this is unlikely due to the results from our global analysis of all the unfolding data (see below).

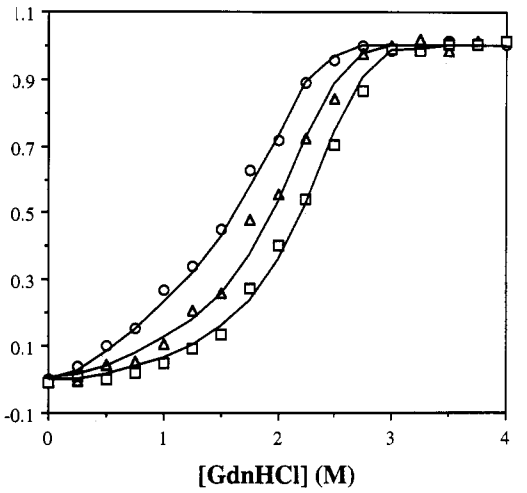

FIGURE 2: Denaturation of R67 DHFR at pH 8.0 monitored by loss of enzyme activity (in units of ΔA_{340} per minute). Data are expressed in terms of F_{app} to facilitate comparison where $F_{app} = (Y_{obs} - Y_N)/(Y_U - Y_N)$, Y_{obs} is the enzyme activity at a particular GdnHCl concentration, and Y_N and Y_U are the calculated values for the native and unfolded forms, respectively, at the same denaturant concentration. For these enzyme activity measurements, Y_U is essentially zero. ○, △, and □ points correspond to 1.0, 5.0, and 10.0 μM tetramer, respectively. The theoretical curves shown were generated by fitting the unfolding data to BIOEQS as described under Results. Best fit values are listed in the text.

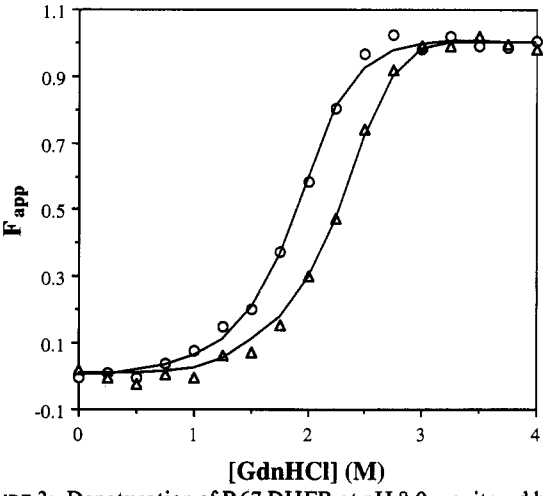

FIGURE 3: Denaturation of R67 DHFR at pH 8.0 monitored by loss of molar ellipticity at 217 nm. Data are expressed in terms of F_{app} to facilitate comparison. ○ and △ points correspond to 1.0 and 5.0 μM tetramer, respectively. The theoretical curves shown were generated from fitting the unfolding data to BIOEQS as described under Results. Best fit values are listed in the text.

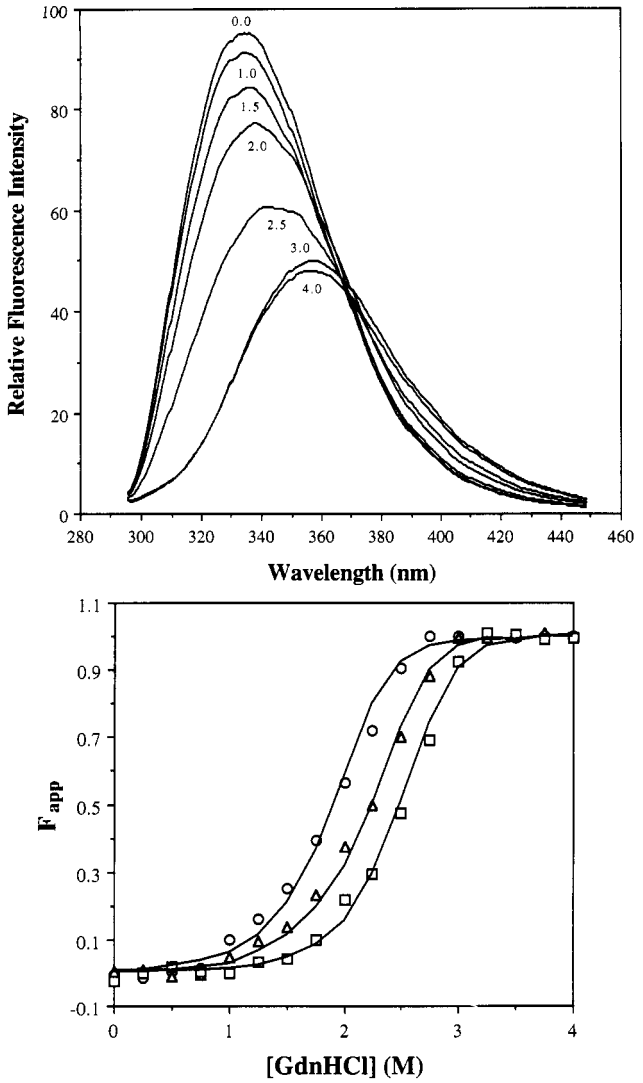

FIGURE 4: (A, top) Fluorescence emission spectra for 5 μM R67 DHFR equilibrated in various concentrations of GdnHCl at pH 8.0, excitation at 290 nm. GdnHCl concentrations are noted near the appropriate curve. (B, bottom) Fluorescence emission at 340 nm was replotted as a function of GdnHCl concentration. Data are expressed in terms of F_{app} to facilitate comparison. ○, △, □ points correspond to 1.0, 5.0, and 10.0 μM tetramer, respectively. The theoretical curves shown were generated from fitting the unfolding data to BIOEQS as described under Results. Best fit values are listed in the text.

Equilibrium folding monitored by fluorescence displays an overall decrease in fluorescence intensity as well as a shift of the peak maximum to higher wavelengths as shown in Figure 4A. Denaturation curves, presented in Figure 4B, are also protein concentration dependent. Notably the fluorescence curves are not biphasic. We might expect to observe two transitions as the two tryptophans which occur per monomer in R67 DHFR are located at two different subunit interfaces. This is apparent from Figure 1, in which W45 and W145, as well as the symmetry related residues W245 and W345, occur at the monomer–monomer interfaces. Using the symmetry operator, W38 and W338 can be envisioned to occur at one dimer–dimer interface; W138 and W238 will occur at the second symmetry related dimer–dimer interface. Why then doesn't fluorescence monitor the T ⇄ 2D transition since we previously used fluorescence to monitor this equilibrium as a function of pH (Nichols et al., 1993)? Perhaps the amplitude of the T ⇄ 2D signal is much smaller than that describing 2D ⇄ 4U.

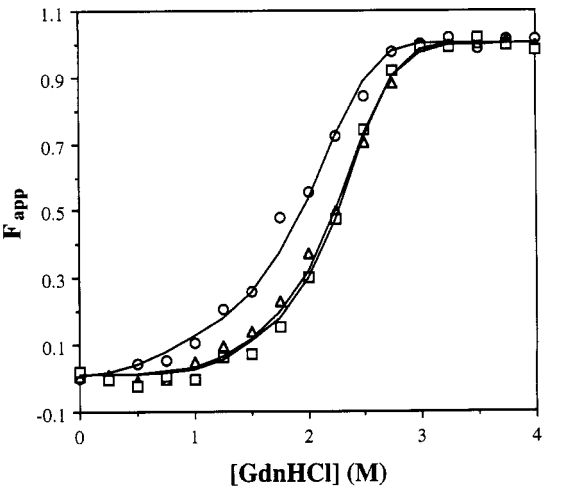

FIGURE 5: Comparison of unfolding in R67 DHFR at pH 8.0. ○, △, □ points correspond to enzyme activity, fluorescence, and molar ellipticity monitored at 5 μM tetramer.

The denaturation curves monitoring changes in fluorescence and secondary structure (CD) overlap, suggesting the same transition is being monitored. For ease of comparison, plots for enzyme activity, fluorescence, and CD data collected at 5 μM tetramer are all presented in Figure 5. Loss of enzyme activity precedes loss of fluorescence and secondary structure. From the nonsuperimposable nature of the unfolding curves determined by these three techniques, equilibrium folding does not follow a two-state model at pH 8.0.

Global Fitting of GdnHCl Denaturation Data to BIOEQS. Our equilibrium data indicate a stable intermediate occurs during folding. Since changes in enzyme activity and fluorescence/CD signals both display protein concentration dependence, two different bimolecular reactions must be occurring. The simplest model that fits these observations is T ⇄ 2D ⇄ 4U. Therefore global fitting of all the GdnHCl induced unfolding data sets obtained by monitoring enzyme activity, fluorescence, and CD was performed using this model and the computer program BIOEQS (Royer, 1993). This program uses a numerical algorithm to solve simultaneous free energy equations. Best fit values are as follows: ΔG_{H_2O} for the transition monitoring the fluorescence and CD signals (2D ⇄ 4U) equals −12.35 kcal/mol (−11.44 to −13.78 kcal/mol, 67% confidence interval) while the ΔG_{H_2O} describing the overall transition T ⇄ 4U is −34.33 kcal/mol (−32.91 to −34.54, 67% confidence interval). Slopes (M_G values) for these transitions are 2.77 (2.38–3.21, 67% confidence interval) and 6.54 kcal mol^{-1} M^{-1}, respectively. The slope measures the cooperativity of the folding reaction.

If K_T describes T ⇄ 2D and equals [D]^2/[T] while K_D describes D ⇄ 2U and equals [U]^2/[D], then the overall transition T ⇄ 4U can be described by an equilibrium constant K_{TD} which equals [U]^4/[T] or $K_T K_D^2$. Therefore a ΔG_{H_2O} of −9.63 kcal/mol corresponding to the T ⇄ 2D transition can be calculated since $\Delta G_{H_2O\ (T \rightleftarrows 4U)} = 2\ \Delta G_{H_2O\ (D \rightleftarrows 2U)} + \Delta G_{H_2O\ (T \rightleftarrows 2D)}$.

From these ΔG_{H_2O} values, fractional populations were calculated for tetramer, dimer, and unfolded monomer as a function of GdnHCl concentration at a total protein concentration of 5 μM. The results are shown in Figure 6. The fractional population plot allows direct comparison of the CD/fluorescence data with the calculated unfolded monomer fraction. The plots coincide quite well (not shown), indicating the CD/fluorescence data predominately describe the equilibrium between 2D and 4U and contain very little information

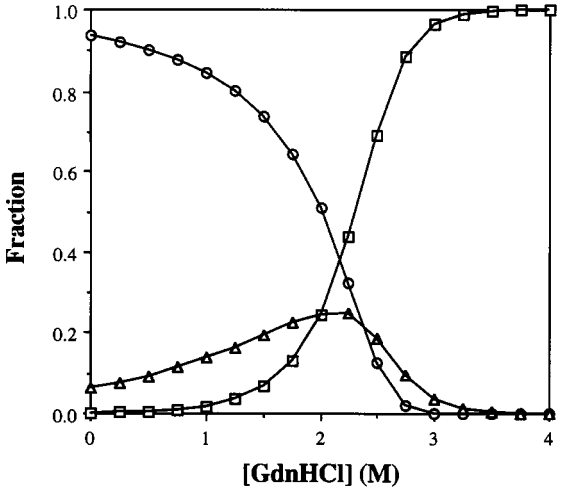

FIGURE 6: Predicted fractional populations of tetramer (○), dimer (△), and unfolded monomer (□) as a function of GdnHCl concentration for a total protein concentration of 5 μM. Eight data sets containing the enzyme activity, CD, and fluorescence data at three different protein concentrations were fit globally using BIOEQS (Royer et al., 1992) as described in the text. The resulting ΔG_{H_2O} values then allowed calculation of this fractional population plot.

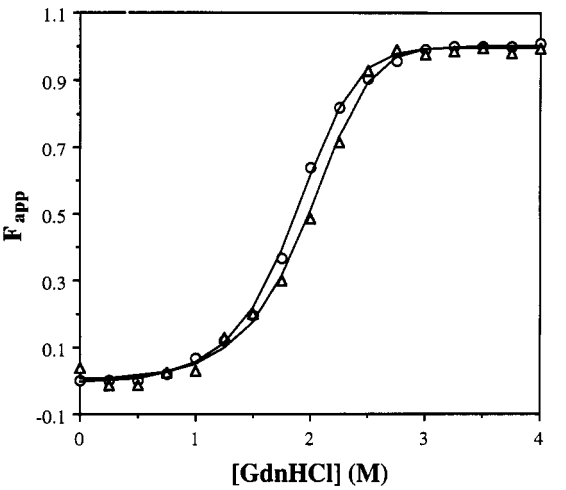

FIGURE 7: Denaturation of dimeric, reduced H62C R67 DHFR at pH 5.0 and 8.0. Data are expressed in terms of F_{app} to facilitate comparison. ○ and △ points correspond to 10 μM H62C dimer at pH 5.0 and 8.0, respectively. Data are the average of two separate experiments. The theoretical curves shown were generated by fitting the folding data to eq 4 in Reece et al. (1991). Best fit values are listed in Table 1.

about the T ⇄ 2D equilibrium. In a parallel fashion, the tetramer fraction plot and the inverse of the enzyme activity plot overlay quite well (not shown); this result indicates the enzyme activity data predominately describe the T ⇄ 2D equilibrium.

Sedimentation Equilibrium in GdnHCl Detects a Dimeric Intermediate. Sedimentation equilibrium studies were undertaken to assess the prediction from spectroscopic and activity measurements that a stable dimeric intermediate was present in the unfolding of R67 DHFR. Sedimentation equilibrium data were obtained at 1, 2, and 3 M GdnHCl. The data from these experiments were first analyzed in terms of a single species to obtain weight average molecular weights. Values of 31 850, 28 750, and 15 080 were obtained for the enzyme in 1, 2, and 3 M GdnHCl, respectively. Previous analyses of R67 DHFR at pH 8.0 in the absence of denaturants yielded a molecular weight of 33 000 (Nichols et al.,1993), which compares well with a molecular weight of 33 720 from the amino acid sequence.

Analysis of the data obtained in 1 M GdnHCl in terms of the number of molecular species indicated that only tetrameric and dimeric R67 DHFR were needed to account for the concentration distribution at sedimentation equilibrium. For the data in 2 M GdnHCl, a model containing terms for monomeric, dimeric, and tetrameric species was required for a minimum in χ^2. Finally, in 3 M GdnHCl, a two term model including monomeric and tetrameric R67 DHFR was required to give a minimum in χ^2. In spite of the assumptions inherent in the sedimentation approach, these results provide strong evidence for the existence of dimeric R67 DHFR in the presence of intermediate GdnHCl concentrations. Moreover, the trends from these analyses are qualitatively consistent with the results obtained from the global analysis of protein unfolding monitored by spectroscopic and enzyme activity measurements.

Attempts to analyze these data in terms of equilibrium constants directly (Nichols et al., 1993) yielded mixed results, however. For the data obtained in 1 M GdnHCl, a dimer–tetramer equilibrium dissociation constant of 2.5×10^{-6} M ($2.0–3.0 \times 10^{-6}$ M, 65% confidence intervals) was obtained. In 3 M GdnHCl, analysis yielded a monomer–tetramer equilibrium dissociation constant of 2.08×10^{-13} M^3 ($1.8–2.36 \times 10^{-13}$ M^3, 65% confidence intervals). The data for sedimentation equilibrium in 2 M GdnHCl consistently gave a lower χ^2 for the inclusion of terms for monomer, dimer, and tetramer, but the confidence intervals on the equilibrium constants from this analysis were too large to establish unequivocally that this model provided a unique description of the data. In all three cases, however, the values of χ^2 were identical to the analyses described above in terms of the number of molecular species present under various denaturation conditions.

Table 1: Fitting Parameters for Unfolding of Dimeric R67 DHFR Monitored by Fluorescence

enzyme	pH	ΔG_{H_2O} (kcal mol^{-1})	M_G (kcal mol^{-1} M^{-1})
10 μM[a] H62C R67 DHFR dimer	5	−12.3 ± 0.3	−3.18 ± 0.14
10 μM[a] H62C R67 DHFR dimer	8	−12.4 ± 0.3	−3.09 ± 0.14
6 μM[a,b] native R67 DHFR	5	−13.2 ± 0.5	−3.51 ± 0.24

[a] Protein concentration expressed as dimer. [b] Data from Reece et al. (1991).

Equilibrium Folding in a Stable Dimeric H62C Mutant R67 DHFR. Histidine 62 and 362 occur at one dimer–dimer interface and His162 and His262 occur at the second symmetry related dimer–dimer interface (see Figure 1; Matthews et al., 1986; Nichols et al., 1993; Xuong, Narayana, and Matthews, personal communication). Our pH studies have shown that protonation of His62 (pK_a = 6.84) and dissociation of active tetramer to inactive dimer are linked processes (Nichols et al., 1993). Therefore a H62C mutation was constructed to stabilize tetrameric R67 DHFR via disulfide bond formation (Howell et al., manuscript in preparation). Disulfide bonds do form, albeit slowly and at high protein concentrations. However, under reducing conditions, H62C R67 DHFR is dimeric. This mutant protein serves as a control by allowing us to monitor unfolding in a dimeric species at pH 5.0 and 8.0 to determine if pH affects dimer folding.

Figure 7 depicts folding curves monitored by fluorescence for H62C R67 DHFR at pH 5.0 and 8.0. Best fit values for the folding curves are listed in Table 1. When the ΔG_{H_2O} values for dimeric H62C R67 DHFR are compared to an average ΔG_{H_2O} for native, dimeric R67 DHFR, no differences

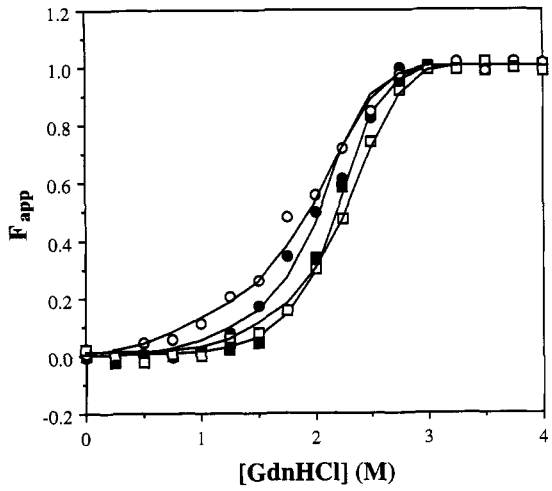

FIGURE 8: Comparison of denaturation in tetrameric R67 DHFR in the presence and absence of 60 μM NADPH. ● and ■ points correspond to denaturation of 5 μM tetramer in the presence of 60 μM NADPH monitored by enzyme activity and molar ellipticity. Data in the presence of NADPH are the average of two separate experiments. ○ and □ points correspond to unfolding of 5 μM tetramer monitored by enzyme activity and molar ellipticity. The theoretical curves shown were generated by fitting the unfolding data to BIOEQS. Best fit values are listed under Results.

are found (within experimental error). Further, there are no significant differences in the unfolding curves for H62C R67 DHFR at pH 5 and 8, indicating that pH has no effect on unfolding monitored by fluorescence in this pH range. These results are consistent with the mutation occurring on the surface of dimeric R67 DHFR.

A comparison of ΔG_{H_2O} values for dimeric H62C R67 DHFR (–12.4 kcal/mol at pH 8.0) with the fluorescence/molar ellipticity transitions in tetrameric native, R67 DHFR (ΔG_{H_2O} = –12.35 kcal/mol) are essentially the same. This observation lends further support to our model describing denaturation of tetramer where fluorescence and CD transitions monitor the 2D $\rightleftarrows$ 4U equilibrium.

Effect of Adding NADPH on the Folding Transition. Addition of 60 μM NADPH (approximately 20 times the K_m value; Reece et al., 1991) to the denaturation conditions for native R67 DHFR at pH 8 resulted in a shift of the curve toward the folded state as well as an increase in the cooperativity (slope) of the reaction (see Figure 8). The data were fit globally using BIOEQS, and best fit parameters are ΔG_{H_2O} = –12.79 kcal mol^{-1} (–10.53 → –14.45 kcal mol^{-1}, 67% confidence interval) and M_G = 3.24 kcal mol^{-1} M^{-1} (2.30 → 3.71 kcal mol^{-1} M^{-1}, 67% confidence interval) for the transition monitored by CD and ΔG_{H_2O} = –35.86 kcal mol^{-1} (–35.22 → –36.22 kcal/mol, 67% confidence interval) and M_G = 7.46 kcal mol^{-1} M^{-1} for the overall transition. The overall transition is shifted such that the folded state is stabilized by –1.53 kcal mol^{-1}. These results indicate addition of 60 μM NADPH stabilizes tetramer and, by mass action, the dimeric intermediate as well.

A dimeric intermediate might be stabilized directly by addition of 60 μM NADPH since dimeric H62C R67 DHFR is partially active with a k_{cat} of 0.034 ± 0.002 s^{-1}, $K_{m\ (DHF)}$ = 36 ± 4 μM, and $K_{m\ (NADPH)}$ = 74 ± 6 μM at pH 7.0. To investigate this possibility, folding curves for dimeric H62C R67 DHFR in the presence or absence of 60 μM NADPH were measured using CD techniques. While the midpoint for the curve containing dimeric H62C R67 DHFR + 60 μM NADPH was displaced to slightly higher GdnHCl concentrations, the ΔG_{H_2O} was within experimental error when compared

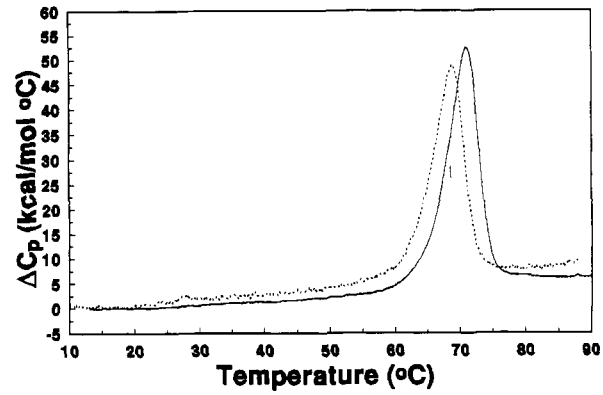

FIGURE 9: Microcalorimetry scans for 148 μM native R67 DHFR at pH 8.0. The first melting scan is shown by the solid line and the cooling scan by the dotted line. Calculated T_m and ΔH values are given under Results.

to the ΔG_{H_2O} describing the apo dimer conditions (data not shown).

Effect of Bis-ANS Addition. Bis-ANS, a dimer of the dye ANS, has been found to bind to hydrophobic areas in proteins (Palleros et al., 1993; Bychkova et al., 1992). In particular, it binds tightly to molten globule states. To determine if such an intermediate occurs during unfolding of tetrameric R67 DHFR, 7 μM bis-ANS was added to the denaturation conditions. Using an excitation wavelength of 394 nm, emission scans for bis-ANS + 5 μM protein + GdnHCl were compared to emission scans for bis-ANS only. No difference in emission maximum was noted, indicating bis-ANS is not bound. If folded monomer were a stable intermediate during unfolding, bis-ANS binding might have been expected since hydrophobic residues in β-strands B–D would have been exposed upon loss of the intersubunit β-barrel and concurrent formation of folded monomer (Matthews et al., 1986).

Microcalorimetry Studies of R67 DHFR. Thermal denaturation of R67 DHFR at pH 5.0 has been shown to be fully reversible by Zhuang et al. (1993) as 94% activity is retained after two cycles of heating and cooling. T_m values of 60.6 and 60.8 °C are observed for the first and second heating cycles, respectively, and a ratio of $\Delta H_{calorimetric}$ to $\Delta H_{van't\ Hoff}$ is 95.38 kcal mol^{-1} / 98.79 kcal mol^{-1} = 0.96. Denaturation in dimeric R67 DHFR can be described by a two-state process as the melting curves are symmetrical and the ratio of $\Delta H_{calorimetric}$ to $\Delta H_{van't\ Hoff}$ is essentially identical to 1.[4]

Thermal denaturation in tetrameric R67 DHFR (pH 8.0) is also reversible as 92% of the activity remains after two cycles of heating and cooling (Figure 9). T_m values of 70.95 °C and 70.65 °C are observed for the first and second heating cycles, and a ratio of $\Delta H_{calorimetric}$ to $\Delta H_{van't\ Hoff}$ (first cycle) is 307.00 kcal mol^{-1}/146.60 kcal mol^{-1} = 2.09.[5] The occurrence of intermediates in the folding process at pH 8.0 is indicated by the asymmetric endotherms and a $\Delta H_{calorimetric}/\Delta H_{van't\ Hoff}$ ratio greater than 1.

DISCUSSION

Equilibrium Folding in Dimeric R67 DHFR is a Two-State Process. We have previously investigated folding in dimeric R67 DHFR at pH 5.0 using equilibrium methods (Reece et al., 1991). Folding is fully reversible in GdnHCl

[4] To calculate $\Delta H_{calorimetric}$, the dimer molecular weight was used. If the monomer molecular weight is used, the ratio of $\Delta H_{calorimetric}/\Delta H_{van't\ Hoff}$ will be 2.

[5] To calculate $\Delta H_{calorimetric}$, the tetramer molecular weight was used.

and can be described by the two-state model

$$D \overset{K}{\rightleftarrows} 2U$$

where D is dimer, U is unfolded monomer, and $K = [U^2]/[D]$. Folding in dimeric R67 DHFR is protein concentration dependent and, within experimental error, absorbance, fluorescence and CD measurements all monitor the same unfolding/refolding transition. An average ΔG_{H_2O} of −13.9 kcal/mol was calculated. Inspection of the dimer structure indicates β-strands B–D from one monomer associate with β-strands from the second monomer, forming a third β-barrel structure. As the third β-barrel occurs at the monomer–monomer interface, it may either help stabilize dimeric R67 DHFR and/or loss of this structure may destabilize folded monomer.

Equilibrium Folding in Tetrameric R67 DHFR at pH 8.0 Is Not a Two-State Process. While loss of protein fluorescence and secondary structure due to GdnHCl induced denaturation are coincident processes within experimental error (Figures 3 and 4B), loss of enzyme activity monitors an earlier transition. The nonoverlapping character of these transitions indicates the occurrence of at least one folding intermediate at pH 8.0. The simplest folding mechanism consistent with our data is $T \rightleftarrows 2D \rightleftarrows 4U$.

Unfolding/refolding monitored by decreasing enzyme activity is protein concentration dependent and describes loss of the active site pore upon dissociation of tetramer. In support of this model, our previous studies have indicated a pH-dependent dissociation of tetramer into two dimers with a K_T value of 9.72 nM (Nichols et al., 1993). This K_T value corresponds to a ΔG of −10.85 kcal mol^{-1}. The ΔG_{H_2O} calculated for the $T \rightleftarrows 2D$ transition in this study is −9.63 kcal/mol, in fair agreement with the value calculated independently.

As noted above, equilibrium folding studies of native, dimeric R67 DHFR at pH 5.0 yield an average ΔG_{H_2O} value of −13.9 kcal mol^{-1} using fluorescence, CD, and absorbance measurements. This value agrees fairly well with the transition in native R67 DHFR monitored by fluorescence and CD at pH 8.0 ($\Delta G_{H_2O} = -12.35$ kcal/mol) as well as the values calculated for the mutant dimeric H62C R67 DHFR ($\Delta G_{H_2O} = -12.3$ and −12.4 kcal/mol at pH 5 and 8). The reasonable agreement of these values further supports our model where loss of CD and fluorescence signals monitors the $2D \rightleftarrows 4U$ equilibrium at pH 8.0 in folding of tetrameric R67 DHFR.

Support for the prediction from global analyses of spectroscopic and enzyme activity measurements with increasing GdnHCl concentration that dimers are intermediates in the denaturation of R67 DHFR comes from sedimentation equilibrium studies. Analysis of sedimentation data in the presence of 1 M GdnHCl in terms of the number of unique molecular weight components present at equilibrium requires both tetrameric and dimeric species. Alternatively, data obtained in 3 M GdnHCl require only monomeric and tetrameric species to account for the sedimentation equilibrium results. A model containing terms for monomers, dimers, and tetramers yielded the lowest χ^2 value for sedimentation equilibrium data obtained for R67 DHFR in 2 M GdnHCl. This result is in agreement with the predictions from global analysis (Figure 6), which shows that all three species are significantly present at this level of denaturant. Generally, the agreement that is seen for the distribution of molecular species present at various denaturant concentrations is quite good in view of the simplifying assumptions used in this analysis such as the effects of quaternary structure and GdnHCl on the partial specific volume and specific extinction coefficient for various R67 DHFR species. Taken together, these results provide experimental support for the presence of dimers in the denaturation of R67 DHFR.

We find no evidence for folded monomer as an intermediate species in unfolding of tetrameric R67 DHFR since the transitions monitored by fluorescence and CD are not biphasic. Further, a consistent ΔG_{H_2O} is calculated over a 10-fold change in protein concentration. These results indicate that folding and dimerization are tightly coupled events.

Unfolding of R67 DHFR$_{double}$. In a previous study, we duplicated the R67 DHFR gene as a first step toward construction of an asymmetric, fully active, monomeric R67 DHFR (Zhuang et al., 1993). The resulting protein, R67 DHFR$_{double}$, is fully active as a dimer, and a pH-dependent dimer ⇄ two monomers equilibrium is observed. The latter is comparable to the tetramer ⇄ two dimers equilibrium occurring in native R67 DHFR. Unfolding of monomeric R67 DHFR$_{double}$ at pH 5.0 is fully reversible. Since both the $D \rightleftarrows 2M$ and $M \rightleftarrows U$ transitions are reversible processes in R67 DHFR$_{double}$, we were surprised to find that unfolding of R67 DHFR$_{double}$ at pH 8.0 (presumably $D \rightleftarrows 2M \rightleftarrows 2U$) is only partially reversible as 38% of the enzyme activity is restored upon dialysis (unpublished data). This result suggests that the unfolding mechanism may instead be $D \rightleftarrows 2M^* \rightleftarrows 2U$, where M* is not equivalent to the monomeric species found at pH 5.0; any structural differences introduced by the covalent linkage of the C-terminus of monomer 1 to the N-terminus of monomer 2 could then affect the ability of R67 DHFR$_{double}$ to reach M* as a folding intermediate.

In a parallel fashion, unfolding in native R67 DHFR may not be as simple as modeled above. In particular, the dimeric folding intermediate may not be identical with the dimer in the crystal structure (Matthews et al., 1986). Thus the unfolding mechanism in R67 DHFR might be better described by $T \rightleftarrows 2D^* \rightleftarrows 4U$, where D* is a dimeric species that is not equivalent to the dimeric crystal structure. If W38, 138, 238, 338 (normally at the dimer–dimer interfaces) were buried in D*, this model could explain why biphasic transitions are not observed when protein fluorescence is monitored (Figure 4). This model could also explain why addition of 60 μM NADPH does not significantly affect unfolding of dimeric H62C R67 DHFR.

Perspective. The $\Delta G_{H_2O}°$ of −34.33 kcal/mol calculated for the overall $T \rightleftarrows 4U$ transition in R67 DHFR indicates excellent stability as a $\Delta G_{H_2O}°$ of −16.1 or −15.4 kcal/mol has been observed for tetrameric melittin (Wilcox & Eisenberg, 1992; Degrado et al., 1981), a $\Delta G_{H_2O}°$ of −22.5 kcal/mol has been calculated for α_4, a designed four-helix bundle protein (Regan & Degrado, 1988), a $\Delta G_{H_2O}°$ of −21.6 kcal/mol has been measured for tetrameric human platelet factor 4 (pH 5), and a $\Delta G_{H_2O}°$ of −38 kcal/mol has been estimated for tetrameric bovine platelet factor 4 (pH 7; Mayo & Chen, 1989).

Model studies in oligomeric proteins have delineated basically two different types of folding mechanisms. In the first type, folding in an oligomer displays essentially two-state behavior, i.e., *stable* folding intermediates are *not* detected. Examples of this type of behavior have been proposed for dimeric transcription factor LFB1 (De Francesco et al., 1991), dimeric gene V protein of bacteriophage f1 (Liang & Terwillinger, 1991), and tetrameric melittin (Wilcox & Eisenberg, 1992). A second type of folding mechanism *does* detect stable intermediates in unfolding of oligomers. Intermediates are folded *n*-monomers (where $n = 1, 2, 3$, etc.);

molten globule states, when identified, are monomeric. This type of behavior is proposed for dimeric aspartate aminotransferase (Herold & Kirschner, 1990), dimeric adenosine cyclic 3′5′-phosphate receptor protein (Cheng et al., 1993), heterodimeric luciferase (Ziegler et al., 1993; Clark et al., 1993), trimeric P22 tailspike protein (Fuchs et al., 1991), tetrameric lactate dehydrogenase (Smith et al., 1991; Badcoe et al., 1991), tetrameric platelet factor 4 (Mayo et al., 1992), tetrameric pyruvate oxidase (Risse et al., 1992), and tetrameric phosphofructokinase (Deville-Bonne et al., 1989; Teschner & Garel, 1989).

R67 DHFR appears to blend both categories as a stable dimeric intermediate is observed while a stable monomeric intermediate is not. This pattern is consistent with the crystal structure and solution studies. Dimeric R67 DHFR is a stable species as it has been observed at pH 5.0 (Nichols et al., 1993) and has been crystallized from 2-methyl-2,4-pentanediol (Matthews et al., 1986). In contrast, monomeric R67 DHFR would not be predicted to be stable as inspection of the dimer structure indicates β-strands B–D from one monomer associate with the equivalent β-strands from the second monomer, forming a third β-barrel structure at the monomer–monomer interface. The interface β-barrel may help stabilize dimeric R67 DHFR and/or loss of this structure may destabilize folded monomer.

ACKNOWLEDGMENT

We thank Dave Matthews, Narendra Narayana, and Nguyen-huu Xuong for sharing their crystal structure data, Cathy Royer for a copy of BIOEQS and for her help in getting it to work, Cynthia Peterson for helpful discussions and critical reading of the manuscript, and Charles Linn for his excellent technical assistance.

REFERENCES

Badcoe, I. G., Smith, C. J., Wood, S., Halsall, D. J., Holbrook, J. J., Lund, P., & Clarke, A.R. (1991) *Biochemistry 30,* 9195–9200.

Bychkova, V. E., Berni, R., Rossi, G. L., Kutyshenko, V. P., & Ptitsyn, O. B. (1992) *Biochemistry 31,* 7566–7571.

Cheng, X., Gonzalez, M. L., & Lee, J. C. (1993) *Biochemistry 32,* 8130–8139.

Clark, A. C., Sinclair, J. F., & Baldwin, T. O. (1993) *J. Biol. Chem. 268,* 10773–10779.

De Francesco, R., Pastore, A., Vecchio, & Cortese (1991) *Biochemistry 30,* 143–147.

Degrado, W. F., Kexdy, F. J., & Kaiser, E. T. (1981) *J. Am. Chem. Soc. 103,* 679–681.

Deville-Bonne, D., Le Bras, G., Teschner, W., & Garel, J.-R. (1989) *Biochemistry 28,* 1917–1922.

Fuchs, A., Seiderer, C., & Seckler, R. (1991) *Biochemistry 30,* 6598–6604.

Gittleman, M. S., & Matthews, C. R. (1990) *Biochemistry 29,* 7011–7020.

Herold, M., & Kirschner, K. (1990) *Biochemistry 29,* 1907–1913.

Jaenicke, R. (1991) *Biochemistry 30,* 3147–3161.

Janin, J. (1991) *Curr. Opin. Struct. Biol. 1,* 42–44.

Kuwajima, K. (1989) *Proteins: Struct., Funct., Genet. 6,* 87–103.

Liang, H., & Terwillinger, T. C. (1991) *Biochemistry 30,* 2772–2782.

Matthews, D. A., Smith, S. L., Baccanari, D. P., Burchall, J. J., Oatley, S. J., & Kraut, J. (1986) *Biochemistry 25,* 4194–4204.

Mayo, E. H., & Chen, M.-J. (1989) *Biochemistry 28,* 9469–9478.

Mayo, K. H., Barker, S., Kuranda, M. J., Hunt, A. J., Myers, J. A., & Maione, T. E. (1992) *Biochemistry 31,* 12255–12265.

Nichols, R., Weaver, C. D., Eisenstein, E., Blakley, R. L., Appleman, J., Huang, T.-H., Huang, F.-Y., & Howell, E. E. (1993) *Biochemistry 32,* 1695–1706.

Pace, C. N., Shirley, B. A., & Thomson, J. A. (1990) in *Protein Structure: A Practical Approach* (Creighton, T. E., Ed.) Chapter 13, IRL Press, Oxford.

Palleros, D. R., Shi, L., Reid, K. L., & Fink, A. L. (1993) *Biochemistry 32,* 4314–4321.

Reece, L. J., Nichols, R., Ogden, R. C., & Howell, E. E. (1991) *Biochemistry 30,* 10895–10904.

Regan, L., & Degrado, W. F. (1988) *Science 241,* 976–978.

Risse, B., Stempfer, G., Rudolph, R., Mollering, H., & Jaenicke, R. (1992) *Protein Sci. 1,* 1699–1709.

Royer, C. A. (1993) *Anal. Biochem. 210,* 91–97.

Royer, C. A., & Beechem, J. M. (1992) *Methods Enzymol. 210,* 481–505.

Schmid, F. X. (1992) *Curr. Opin. Struct. Biol. 2,* 21–25.

Smith, C. J., Clarke, A. R., Chia, W. N., Atkinson, T., & Holbrook, J. J. (1991) *Biochemistry 30,* 1028–1036.

Teschner, W., & Garel, J.-R. (1989) *Biochemistry 28,* 1912–1916.

Wilcox, W., & Eisenberg, D. (1992) *Protein Sci. 1,* 641–653.

Zhuang, P., Yin., M., Holland, J., Peterson, C. B., & Howell, E. E. (1993) *J. Biol. Chem. 268,* 22672–22679.

Ziegler, M. M., Goldberg, M. E., Chaffotte, A. F., & Baldwin, T. O. (1993) *J. Biol. Chem. 268,* 10869–10765.